Journal of Integrative Neuroscience

J. Integr. Neurosci. **2022**; 21(5): 127
https://doi.org/10.31083/j.jin2105127

Original Research

Transcriptome Evidence Reveals Mitochondrial Unfolded Protein Response Participate in SH-SY5Y Cells Exposed to Manganese

Shixuan Zhang[1,2,†], Li Chen[1,2,†], Tian Chen[1,2], Yuanyuan Zhang[1,2], Junxiang Ma[1,2], Hongyun Ji[1,2], Caixia Guo[1,2], Zhongxin Xiao[3], Jie Li[1,2,*], Piye Niu[1,2,*]

[1]Department of Occupational Health and Environmental Health, School of Public Health, Capital Medical University, 100069 Beijing, China
[2]Beijing Key Laboratory of Environmental Toxicology, School of Public Health, Capital Medical University, 100069 Beijing, China
*Correspondence: lijie46@ccmu.edu.cn (Jie Li); niupiye@ccmu.edu.cn (Piye Niu)
[†]These authors contributed equally.
Academic Editor: Yoshihiro Noda
Submitted: 16 February 2022 Revised: 11 March 2022 Accepted: 14 March 2022 Published: 21 July 2022

Abstract

Background: Overexposure to manganese (Mn) can lead to neurodegenerative damage, resulting in manganism with similar syndromes to Parkinson's disease (PD). However, little is known about changes in transcriptomics induced by the toxicological level of Mn. In this study, we conducted RNA-seq to explore the candidate genes and signaling pathways included by Mn in human SH-SY5Y neuroblastoma cells. **Methods**: The differentially expressed genes (DEGs) between the Mn-treated group and the control group were screened, and weighted gene co-expression network analysis (WGCNA) was employed to identify hub genes. Then, pathway enrichment analyses for those candidate genes were performed in Gene Ontology (GO) and Kyoto Encyclopedia of Genes and Genomes (KEGG). We further validated the concentration- and time-response effects of Mn exposure (0–500 μM, 3–12 h) on mitochondrial unfolded protein response (UPR^{MT}) by real-time quantitative reverse transcription PCR (qRT-PCR). **Results**: The results showed 179 up-regulated differentially expressed genes (DEGs) and 681 down-regulated DEGs after Mn exposure. Based on the intersection of DEGs genes and hub genes, 73 DEGs were related to neurotoxicity. The comprehensive pathway analysis showed Mn had widespread effects on the mitogen-activated protein kinase (MAPK) signaling pathway, unfolded protein response, longevity regulating pathway, inflammatory bowel disease, and mitophagy signaling pathway. After Mn exposure, the expressions of activating transcription factor 3 (ATF3) and C-C motif chemokine ligand 2 (CCL2) increased, while the expressions of C/EBP homologous protein (CHOP), caseinolytic protease P (CLPP), and Lon protease 1 (LONP1) decreased in a concentration- and time-dependent manner. **Conclusions**: Overall, our study suggests that UPR^{MT} is a new sight in understanding the mechanism of Mn-induced neurotoxicity.

Keywords: manganese; neurotoxicity; bioinformatics; candidate genes; mitochondrial unfolded protein response

1. Introduction

Manganese (Mn) is an essential nutrient metal used in various physiological processes, including lipid, protein, and carbohydrate metabolism, especially in neurodevelopment [1]. However, the excessive accumulation of Mn in the central nervous system (CNS) can lead to manganism that features symptomatology similar to Parkinson's disease (PD) [2]. The biological mechanisms of neurotoxic effects induced by Mn include oxidative stress, mitochondria dysfunction, protein folding abnormalities, endoplasmic reticulum stress, autophagy disorders, apoptosis, and impaired metabolism pathways [3,4]. Although mitochondria are the main targets of Mn, the specific mechanism of its neurotoxicity is not known [5,6].

The previous study has shown endoplasmic reticulum unfolded protein response (UPR^{ER}) can be induced by Mn exposure [7], but the evidence of mitochondrial unfolded protein response (UPR^{MT}) participating in the neurotoxicity of Mn is still limited. The proteostasis is surveilled by the UPR^{MT}, an adaptive signal transduction pathway that maintains the fidelity of protein folding in mitochondria [8]. Abnormal accumulation of unfolded or misfolded proteins can cause cellular stress, which may be a driver of human diseases. UPR^{MT} includes nucleo-coding targeted mitochondrial molecular chaperones and proteolytic enzymes, such as heat shock proteins (HSP10, HSP60, and HSP90), LONP1, CLPP, and CHOP. Recent studies have found that the UPR^{MT} plays an important role in the occurrence and development of neurodegenerative diseases [9,10]. The expression of UPR^{MT} genes increased significantly in the frontal cortex of sporadic and familial Alzheimer's disease (AD) patients [11]. Decreased expression of mitochondrial HSP70 in the substantia nigra of the brain in PD patients [12]. However, due to the complexity and diversity of mammalian mitochondrial function, the role and mechanism of UPR^{MT} in human diseases need to be further studied.

To fully explore the molecular participation in Mn neurotoxicity, the transcriptional changes in neurocytes were detected. The appropriate maximum exposure concentration of Mn was selected by cell viability. After the screening of differentially expressed genes (DEGs),

weighted gene coexpression network analysis (WGCNA) was used to identify critical modules and candidate genes to reveal potential biomarkers. The potential biological pathways were explored in Gene Ontology (GO) and Kyoto Encyclopedia of Genes and Genomes (KEGG) databases. Furthermore, we validated the concentration- and time-response effects of Mn on the expression of candidate genes by qRT-PCR in SH-SY5Y cells induced by Mn (0–500 μM, 3–12 h).

2. Materials and Methods

2.1 Cells Culture

The human neuroblastoma cell line SH-SY5Y was purchased from the Cell Resource Center of Peking Union Medical College. The cells were cultured [13] in the high glucose (4.5 g/L D-Glucose) DMEM (Gicbo Inc, 11960044, Grand Island, NE, USA), medium containing 10% fetal bovine serum, 2% L-Glutamine, and 1% sodium pyruvate at 37 °C, 5% CO_2 for 36–48 h. The cells whose density reached 80% (about 8×10^6 cells) were subcultured by treatment with 0.25% trypsin for 1 min, rinsed from the substrate with serum-containing medium, collected by centrifugation at 1000 rpm for 5 min, and seeded into fresh culture dish in a ratio of 1:3.

2.2 Cell Viability Assay

CCK-8 kit (ZOMANBIO Inc., ZP328, Beijing, China) was used to measure the viability of SH-SY5Y cells. A total of 1×10^4 cells in a volume of 100 μL per well were cultured in six replicate wells in a 96-well plate for 24 h and then treated with different concentrations of $MnCl_2$ (0, 62.5, 125, 250, 500, 1000 μM) for 3, 6, and 12 h. Then, 10 μL CCK-8 reagent was added per well with 90 μL DMEM and incubated for 1.5 h at 37 °C. The absorbance was determined at 450 nm using a microplate reader (**Supplementary Fig. 1**).

2.3 RNA-Seq Data Processing and Analysis

According to ISO 10,993–5, the cell viability threshold for the test is >70%, using the statistically significant highest exposure concentration and time compared to the control, for microarray analysis (500 μM $MnCl_2$, 6 h). Then the transcriptomes were detected in 3 treated samples and 3 control samples. Total RNA was quantified by the NanoDrop (Thermo Scientific Inc., ND, USA), and the RNA integrity was assessed using Agilent Bioanalyzer 2100 (Agilent Technologies Inc., G2939AA, Palo Alto, CA, USA). The expression profiles of mRNAs in SH-SY5Y cells were tested by the Agilent Human (4×180K). The sample labeling, microarray hybridization, and washing were performed based on the manufacturer's standard protocols. The arrays were scanned with the Agilent Scanner (Agilent Technologies Inc., G2505C, Palo Alto, CA, USA).

2.4 DEGs Analysis

To eliminate differences between samples, we used a robust multichip average algorithm (RMA), including background correction (removes array auto-fluorescence), quantile normalization (makes all intensity distributions identical), and probe set summarization (calculates one representative value per probe set). After gene expression data processing and normalizing, we used the "limma" package in R (version 4.0.3, https://www.r-project.org/) to screen differentially expressed mRNA, $|FC| \geq 2$ and $p < 0.05$ were selected to be the cutoff criteria.

2.5 Identification of Coexpression Network and Hub Genes

We use the "WGCNA" package in R (version 4.0.3) to analyze the genes [14,15]. The scale-free fitting index of various soft threshold powers (power-value = 0.85) was analyzed by the coexpression network. The nodes with high correlation were placed into a single module, and the genes were clustered together with the module eigengene and intramodular. Then the clustering tree was cut into different modules using dynamic shearing. The hub genes in a module are the genes with the maximum connectedness (KWithin) under the module. The MM value can be obtained by correlation analysis between the expression amount of the gene and the first principal component of the module. At the same time, correlation analysis was conducted between the expression level of this gene and the corresponding phenotypic value, and the final correlation coefficient value was GS. Hub gene is defined as the gene of $|GS| \geq 0.2$ and $|MM| \geq 0.8$ for a specific module.

2.6 Pathway Enrichment Analysis

GO enrichment analysis was used to determine target molecular functions (MF), biological processes (BP), and cellular components (CC) of DEGs. Based on the KEGG database, we performed pathway enrichment analysis for DEGs. For both analyses, Benjamini-Hochberg statistical method, $p < 0.05$ was considered as statistically significant by Cytoscape (version 3.7.2, https://cytoscape.org/) and R (version 4.0.3).

2.7 qRT -PCR Analysiss

Based on the candidate genes, and previous research, we validated the expression of ATF3, CCL2, CHOP, CLPP, HSP10, HSP60, HSP90, and LONP1 by qRT-PCR. We isolated the total RNA from SH-SY5Y cells by the Trizol method (Solarbio Inc., 15596026, Beijing, China). cDNA was synthesized from 1 μg total RNA using the PrimeScript^{TM} RT reagent Kit (TaKaRa Bio Inc., RR047A, Shiga, Japan). Then the 2 μL cDNA was diluted in a total volume of 20 μL according to SYBR Green real-time PCR master mix (TOYOBO Inc., QPS-201, Osaka, Japan), and the expression of crucial genes was measured by the CFX96 Real-Time System (BIO-RAD Inc., Hercules, CA, USA). The primers of mRNAs were listed in **Supplemen-**

tary Table 1. GAPDH was used to normalize the levels of mRNAs. The method of $2^{-\Delta\Delta Ct}$ was used to calculate the relative expression of mRNAs. All results were derived from triplicate experiments and presented as mean $\pm$ SD. $p < 0.05$ was considered significant statistically.

3. Results

3.1 DEGs Responded to Mn Exposure

As shown in Fig. 1, the normalized data were distributed in a symmetrical median, indicating relatively high reliability of the experimental design and data. Among the 19,991 total mRNAs in SH-SY5Y cells exposed to Mn, the Mn-treated group had 860 DEGs ($|FC| \geq 2$ and $p < 0.05$), among which 179 genes up-regulated and 681 genes down-regulated, compared with the control group.

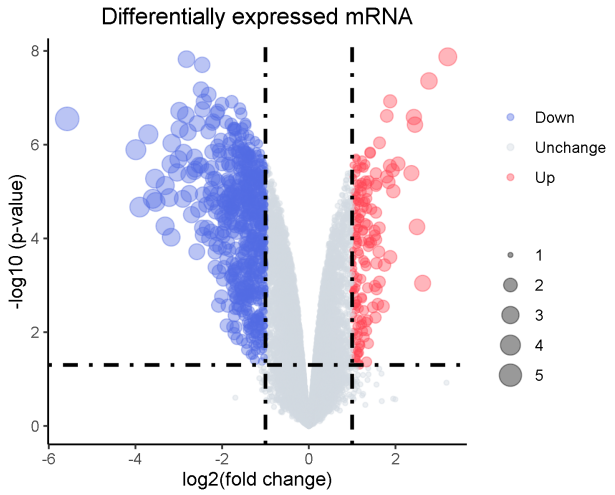

Fig. 1. Differentially expressed genes. The X-axis shows the FC (log-scaled), and Y-axis indicates *p*-values (log-scaled). Red and blue dots represent up-regulated and down-regulated genes, respectively. Grey dots represent non-DEGs. Under the criterion of $|FC| \geq 2$ and $p < 0.05$.

3.2 Candidate Genes Highly Related to Mn Exposure

The first 50% median of absolute deviation was incorporated into the WGCNA. The dynamic tree cutting method was used to identify each module, and the correlation degree was more than 0.75 modules consolidated into 18 modules (Fig. 2A). The merged module correlation diagram was redrawn, and the correlation coefficients between the modules and phenotype were visualized (Fig. 2B). There were 1396 hub genes clustered with the most significant positive correlation, while the "turquoise" module was the most significant negative correlation, with 2843 hub genes aggregated (Fig. 2C,D). Intersection analysis with DEGs showed that after Mn exposure, the expression level of 823 candidate genes changed significantly, with 160 up-regulated genes and 663 down-regulated genes (Fig. 2E). These genes were highly correlated with their corresponding modules and relative traits.

3.3 Pathway Enrichment Analysis of Differentially Expressed Candidate Genes

To clarify the function of the candidate genes, we performed the GO enrichment analysis. The results showed that differentially expressed candidate genes were mainly involved in 10 terms related to neurotoxicity (Fig. 3A), which enriched 73 mRNAs (Fig. 3B,C). By GO enrichment analysis of these genes, the potential biological functions of nerve cell injury were further discussed. The results showed that Mn mainly affected the regulation of neuron death, and mitochondrial functions including regulation of reactive oxygen species biosynthetic process, mitochondrial outer membrane permeabilization, the release of cytochrome c from mitochondria, and apoptotic signaling pathway (Fig. 3D). As mitochondria are the major target of Mn, KEGG pathway enrichment analysis was further performed for genes enriched in mitochondrial-related functions. These genes participated in the MAPK signaling pathway, UPR, longevity regulating pathway, inflammatory bowel disease, and mitophagy (Fig. 3E).

3.4 The Concentration- and Time-Response Relationship between UPR^{MT} Genes and Mn Exposure

Recent studies showed UPR is a new mechanism for neurodegenerative diseases, therefore the expressions of UPR^{MT} genes were further verified by qRT-PCR in SH-SY5Y cells treated with 0–500 μM $MnCl_2$ for 6 h, and 500 μM $MnCl_2$ for 3–12 h. As shown in Fig. 4A, the expressions of ATF3, CCL2, and HSP90 increased, and the expressions of CHOP, CLPP, and LONP1 decreased in a concentration-dependent manner. The expressions of HSP10 and HSP60 increased significantly after Mn exposure, but there was no concentration-response relationship. As shown in Fig. 4B, the expressions of ATF3 and CCL2 increased, while CHOP, CLPP, HSP10, and LONP1 decreased in a time-dependent manner.

4. Discussion

Mn is widely used in industrial production, such as mining, metal smelting, welding, and other fields. Mn can cause neurotoxicity *in vitro* and *in vivo*, leading to manganism, Parkinson-like symptoms, pathologically characterized by the loss of dopaminergic neurons [16]. In this study, we found the expressions of ATF3 and CCL2 increased, while the expressions of CHOP, CLPP, and LONP1 decreased in a concentration- and time-dependent manner after Mn exposure in SH-SY5Y cells. Our results revealed that the UPR^{MT} pathway was involved in neurotoxicity induced by Mn for the first time and mitochondrial proteostasis dysfunction is an important mechanism of neurotoxicity induced by Mn.

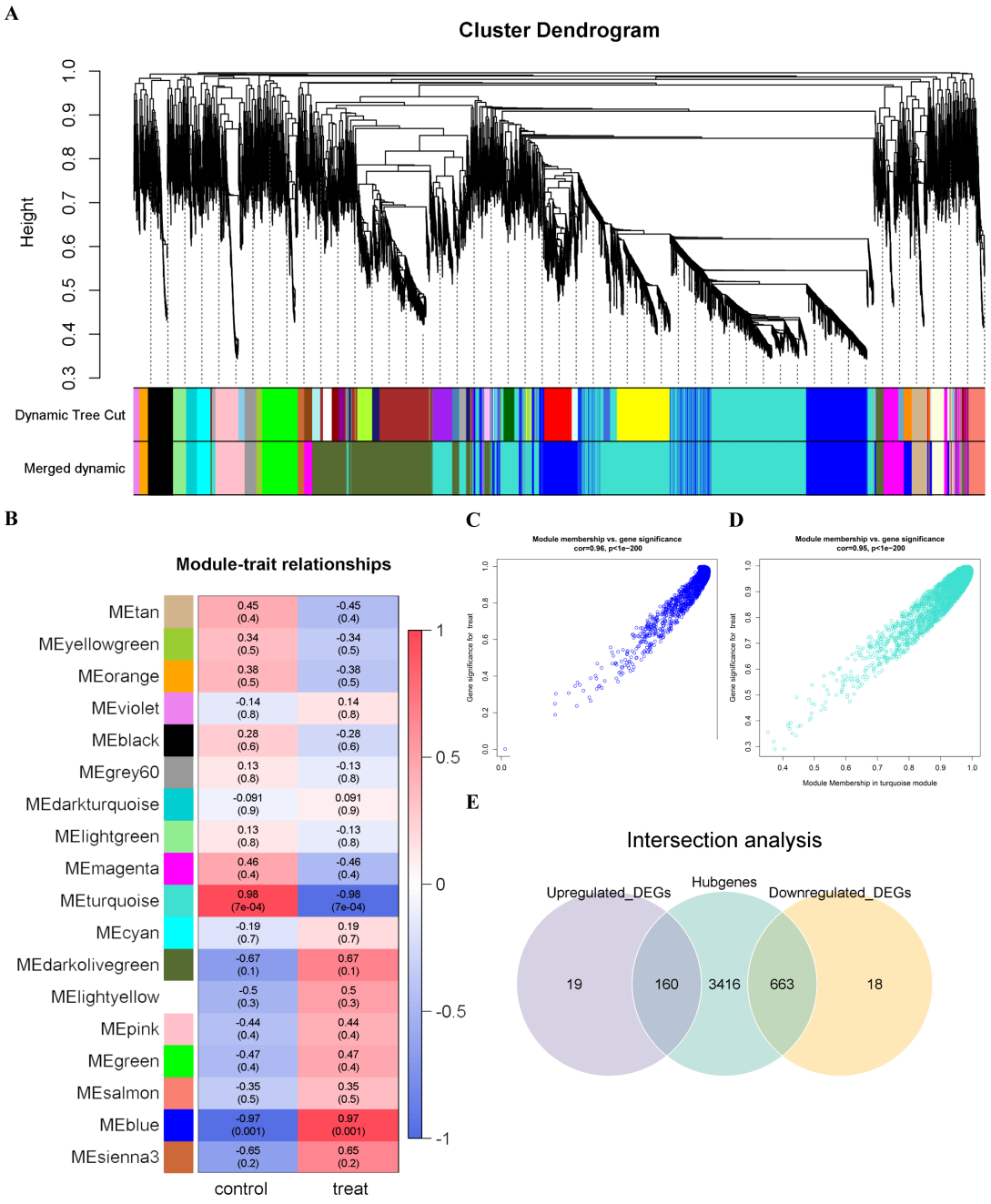

Fig. 2. Visualization of mRNAs expression hierarchical clustering, and gene module partitioning. (A) Clustering of mRNAs, cutting the clustering tree by dynamic shearing into different modules. The cut height was set as 0.75 to merge similar modules. (B) The correlation coefficients between models and phenotype. Red and blue represent positive correlation and negative correlation, respectively. (C) The module with the most significant positive correlation. (D) The module with the most significant negative correlation. Under the criterions of $|GS| \geq 0.2$, $|MM| \geq 0.8$ and $p < 0.05$. (E) The intersection of the up-regulated or down-regulated DEGs with hub genes to obtain candidate genes.

Manganism is most commonly associated with occupational or environmental exposure to Mn, which exhibits neurotoxicity similar to PD and is characterized by cognitive and motor dysfunction. PD is a progressive movement disorder characterized by selective neurodegeneration of dopaminergic neurons in the substantia nigra [17]. Under neurotoxic conditions, Mn has been shown to accumulate in the subcortical structures of the basal ganglia, particularly in the substantia nigra pallidum and striatum. Positron emission tomography imaging in the striatum of brains exposed to Mn has revealed impaired DA transmission, a feature of PD [18]. Proteins related to PD pathogenesis were

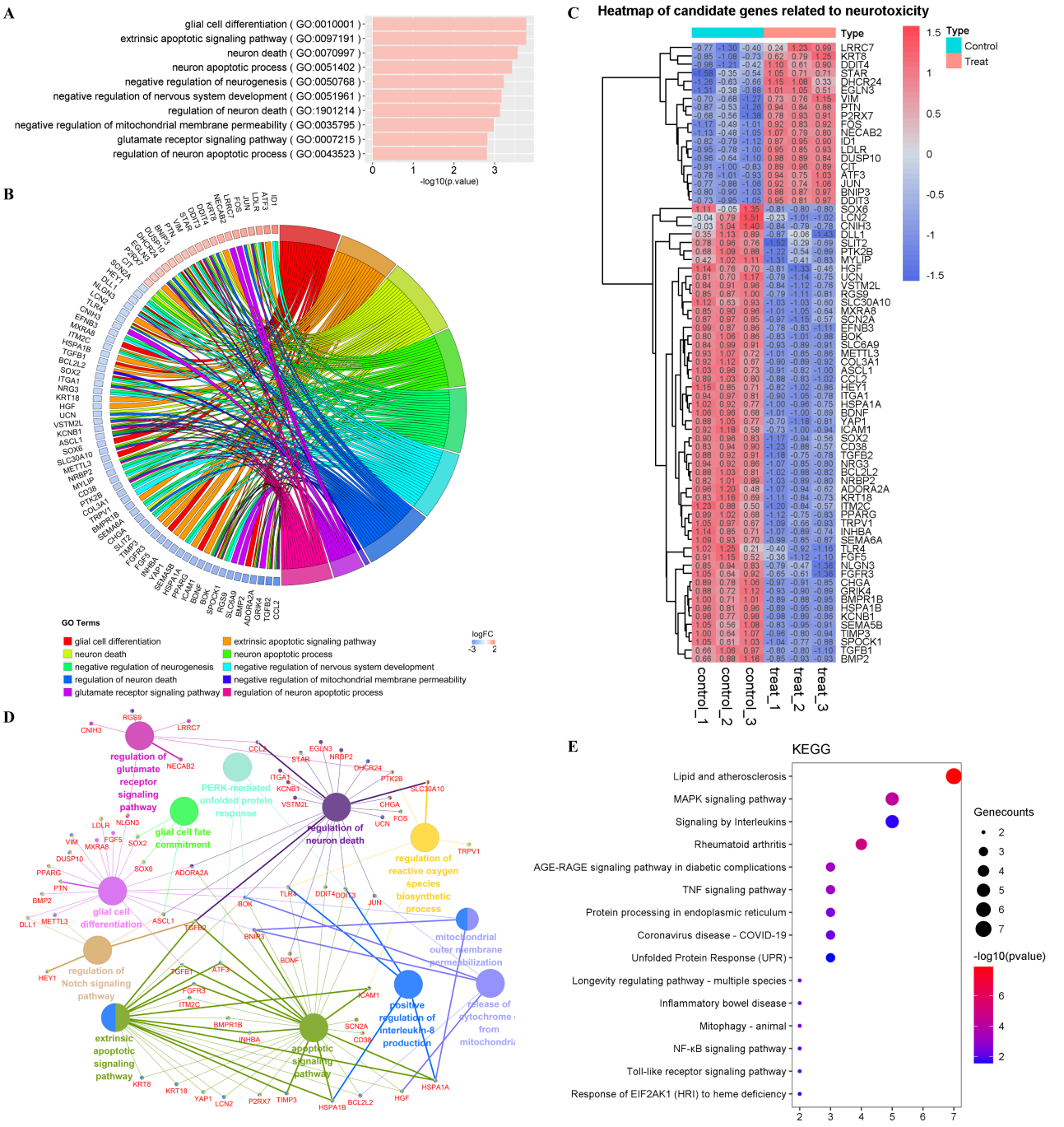

Fig. 3. Identification and functional enrichment of candidate genes. (A) The biological process, hub genes enriched, includes 10 GO terms related to neurotoxicity. The X-axis shows the negative logarithm of the *p*-value, Y-axis shows the name of the GO terms. (B) The hub genes are mainly enriched in biological processes related to neurotoxicity. (C) Heatmap of candidate genes related to neurotoxicity. Red and blue represent positive correlation and negative correlation, respectively. (D) GO enrichment analysis of candidate genes. (E) KEGG enrichment analysis of candidate genes.

accumulated in Mn treated SH-SY5Y cells [19,20]. The human neuroblastoma cell line, SH-SY5Y, is a common model in studies related to neurotoxicity and neurodegenerative diseases [13,21]. Although the SH-SY5Y cell line exhibits multiple genetic aberrations due to its cancer origin, each PD-related gene has at least one copy and the major PD pathways were intact in the SH-SY5Y genome [22]. However, the difference between their transcriptome and that of healthy neurons affects the neurotoxicity of Mn is worth exploring.

PERK, IRE1α, and ATF6α are three endoplasmic reticulum sensors that are activated to maintain protein

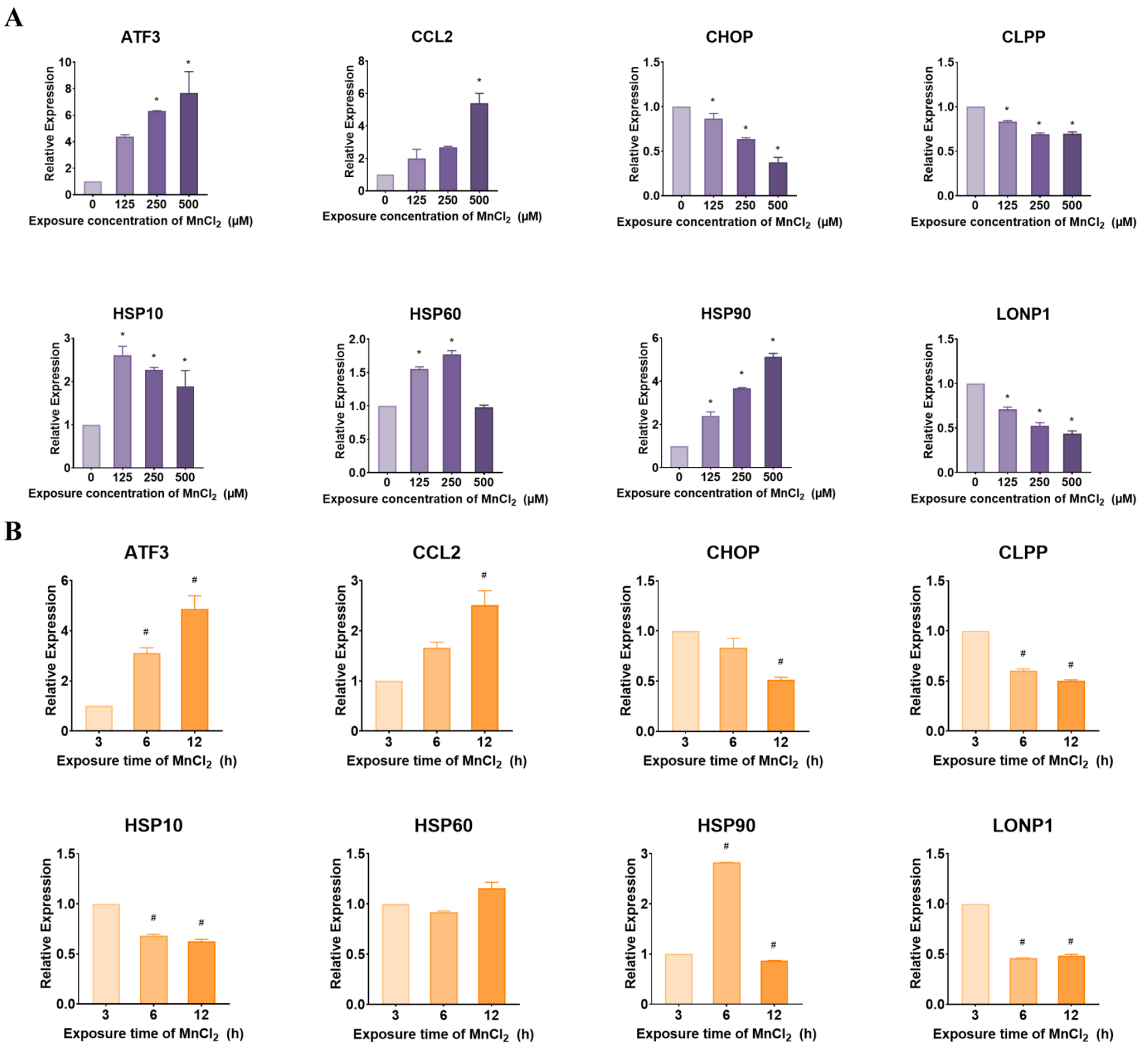

Fig. 4. The expressions of UPR^{MT} related genes after Mn exposure were analyzed by qRT-PCR. Relative mRNAs expressions of mitochondrial functional and structural damage in SH-SY5Y cells exposed to 0, 125, 250, and 500 μM $MnCl_2$ for 6 h (A) and 500 μM $MnCl_2$ for 3, 6, and 12 h (B). Data are expressed as means $\pm$ SD from three independent experiments at least. Statistical significance was assessed using one-way ANOVA. *$p < 0.05$ compared with control. #$p < 0.05$ compared with the group of $MnCl_2$ exposure for 3 h.

homeostasis in cells which can promote apoptosis upon prolonged UPR^{ER} [23]. As compared with UPR^{ER}, the pathways of UPR^{MT} were well characterized and can be initiated to enhance folding and degradation in response to the accumulation of unfolded and aggregated proteins in mitochondria [24]. UPR^{MT} is an adaptive signal transduction pathway that maintains mitochondrial proteostasis. Distinct from the UPR^{ER} mechanism, UPR^{MT} includes a series of nucleo-coding targeted mitochondrial molecular chaperones (HSP10, HSP60, and CHOP) and proteolytic enzymes (LONP1 and CLPP). The expression of UPR^{MT} -related proteins HSP60, LONP1, and CLPP increased significantly in A$\beta_{25\text{-}35}$ treated SH-SY5Y cells. Disruption of UPR^{MT} induced mitochondrial damage, ROS accumulation, and decreased cell viability in SH-SY5Y cells. The expression levels of HSP60 and CLPP have significantly increased in 3 months old AD model mice compared to WT mice, while the expression level of HSP60 was significantly decreased in 9-month-old transgenic mice compared to 3-month-old transgenic mice [21]. The levels of CLPP and HSP60 increased significantly and rapidly in SH-SY5Y cells after 2 h of MPP treatment, indicating that UPR^{MT} was activated, while the levels decreased after 8 h of treatment [25]. Abnormal or prolonged UPR^{MT} activation leads to cells in a state of continuous mitochondrial recovery, which may increase the accumulation of deleterious mitochondrial DNA and directly contribute to the age-related deterioration [26]. Recent studies have also shown UPR^{MT} played a protective role in impaired mitochondria and proteotoxic stress in the pathogenetic process of AD and PD. In the Drosophila melanogaster model of PD, UPR^{MT} can be induced to alleviate mitochondrial dysfunction and neu-

rodegeneration [27]. It has been shown that pink-1 mutation can activate ATFS-1 mediated UPR^{MT} and promote dopamine neuron survival in PD [28], and the mutation of the UPR^{MT} gene causes neuropathy with the same characteristics as PD [29]. Overactivation of UPR^{MT} signaling led to a shortened lifespan of C. elegans and accumulate defective mitochondria in dopaminergic neurons [8]. The treatment of SH-SY5Y cells with either thapsigargin or tunicamycin could induce UPR^{ER}, but the expression of mitochondrial protease LONP1 and mitochondrial chaperone HSP60 was not significantly altered [30]. Previous studies have shown that Mn exposure can lead to UPR^{ER} [31], while the present study confirmed that Mn can also affect UPR^{MT} -related gene expression in SH-SY5Y cells.

Using comprehensive bioinformatics methods and qRT-PCR, we also found ATF3 and CCL2 increased in a concentration- and time-response manner. Both ATF3 and CCL2 participated in regulating the mitochondrial integrated stress response. CCL2 is involved in immunomodulatory and inflammatory processes as a chemokine. Endothelial cell injury upregulates downstream molecules of UPR^{ER}, leading to increased release of CCL2, which may inhibit mitochondrial autophagy [32]. Previous studies showed Mn treatment could dramatically enhance the expression of CCL2 in microglia [33]. ATF3 encodes a cAMP-responsive element-binding (CREB) protein family of transcription factors. But the evidence between ATF3 and Mn exposure is limited. After UPR^{MT} was activated in mouse and human muscle tissues, ATF3, HSP10, HSP60, LONP1, and CLPP expression were elevated to different degrees [34]. HSP10, HSP60, and HSP90 belong to mitochondrial molecular chaperones [35]. We also observed that Mn can activate the expression of heat shock proteins (HSP10, HSP60, and HSP90), which was consistent with a previous study in C. elegans [36]. The above results indicated Mn exposure can partially activate UPR^{MT}. Our results also observed Mn treatment resulted in a concentration- and time-dependent decrease in gene expressions of CHOP, CLPP, and LONP1. CHOP belongs to the CCAAT/enhancer-binding protein (C/EBPs) family and regulates proteins-coding in proliferation, differentiation, and energy metabolism. CHOP is a key protein in endoplasmic reticulum stress and mitochondrial stress. Previous studies showed that Mn exposure could induce CHOP in SH-SY5Y cells and striatal of SD rats [37,38]. The inconsistent results may be due to different treatment concentrations and times of Mn. CLPP and LONP1 as mitochondrial proteases can remove oxidized mitochondrial proteins in the matrix [35]. However, the regulatory pathways behind the decreased expression of partial UPR genes by Mn still need to be studied.

Our results indicated an interesting phenomenon that Mn can simultaneously activate and inhibit gene expression of UPR^{MT}. Although mRNA microarray expression has shown to be highly concordant when re-analyzed with qRT-PCR, these mRNA-encoded proteins should be further investigated by western blot or proteomics analysis to more clearly illustrate the specific effect of Mn on UPR^{MT}. It has been reported that UPR has both protective and apoptotic effects according to different physiological conditions, activation time, and intensity [10]. Moderate activation of UPR can remove the accumulation of misfolded proteins and reduce the toxic effect. However, exceeding the threshold of UPR tolerance may trigger autophagy and lead to apoptosis [31].

5. Conclusions

Our results showed Mn could trigger and inhibit UPR^{MT} simultaneously in nerve cells in a concentration- and time-response manner, which might provide clues to the molecular mechanism of neurotoxicology caused by Mn.

Abbreviations

AD, Alzheimer's disease; ATF3, activating transcription factor 3; CCL2, C-C motif chemokine ligand 2; CHOP, C/EBP homologous protein; CLPP, caseinolytic protease P; CNS, the central nervous system; DEGs, differentially expressed genes; FC, fold change; GO, Gene Ontology; GS, gene significance; HSP10, heat shock protein 10; HSP60, heat shock protein 60; HSP70, heat shock protein 70; HSP90, heat shock protein 90; KEGG, Kyoto Encyclopedia of Genes and Genomes; LONP1, Lon protease 1; MAPK, mitogen-activated protein kinases; MM, module member-ship; Mn, manganese; PD, Parkinson's disease; UPR, unfolded protein response; UPR^{ER}, endoplasmic reticulum unfolded protein response; UPR^{MT}, mitochondrial unfolded protein response; WGCNA, weighted gene coexpression network analysis.

Author Contributions

These should be presented as follows: PN, JL, SZ and LC designed the research study. SZ and LC performed the research. YZ, JM, HJ provided help and advice on validation. SZ, LC and JL analyzed the data. SZ, JL and LC wrote the manuscript. TC, JM, CG and ZX contributed to editorial changes in the manuscript. All authors read and approved the final manuscript.

Ethics Approval and Consent to Participate

Not applicable.

Acknowledgment

Not applicable.

Funding

This research was funded by the National Natural Science Foundation of China, grant number 81973007.

Conflict of Interest

The authors declare no conflict of interest. JL is serving as one of the Guest editors of this journal. We declare that JL had no involvement in the peer review of this article and has no access to information regarding its peer review. Full responsibility for the editorial process for this article was delegated to YN.

Supplementary Material

Supplementary material associated with this article can be found, in the online version, at https://doi.org/10.31083/j.jin2105127.

References

[1] Horning KJ, Caito SW, Tipps KG, Bowman AB, Aschner M. Manganese is Essential for Neuronal Health. Annual Review of Nutrition. 2015; 35: 71–108.

[2] Racette BA, Nelson G, Dlamini WW, Prathibha P, Turner JR, Ushe M, *et al*. Severity of parkinsonism associated with environmental manganese exposure. Environmental Health. 2021; 20: 27.

[3] Zhang Z, Yan J, Bowman AB, Bryan MR, Singh R, Aschner M. Dysregulation of TFEB contributes to manganese-induced autophagic failure and mitochondrial dysfunction in astrocytes. Autophagy. 2020; 16: 1506–1523.

[4] Mehdizadeh P, Fesharaki SSH, Nouri M, Ale-Ebrahim M, Akhtari K, Shahpasand K, *et al*. Tau folding and cytotoxicity of neuroblastoma cells in the presence of manganese oxide nanoparticles: Biophysical, molecular dynamics, cellular, and molecular studies. International Journal of Biological Macromolecules. 2019; 125: 674–682.

[5] Warren EB, Bryan MR, Morcillo P, Hardeman KN, Aschner M, Bowman AB. Manganese-induced Mitochondrial Dysfunction is not Detectable at Exposures below the Acute Cytotoxic Threshold in Neuronal Cell Types. Toxicological Sciences. 2020; 176: 446–459.

[6] Sarkar S, Malovic E, Harischandra DS, Ngwa HA, Ghosh A, Hogan C, *et al*. Manganese exposure induces neuroinflammation by impairing mitochondrial dynamics in astrocytes. NeuroToxicology. 2018; 64: 204–218.

[7] Liu C, Yan D, Wang C, Ma Z, Deng Y, Liu W, *et al*. Manganese activates autophagy to alleviate endoplasmic reticulum stress-induced apoptosis via PERK pathway. Journal of Cellular and Molecular Medicine. 2020; 24: 328–341.

[8] Martinez BA, Petersen DA, Gaeta AL, Stanley SP, Caldwell GA, Caldwell KA. Dysregulation of the Mitochondrial Unfolded Protein Response Induces Non-Apoptotic Dopaminergic Neurodegeneration in C. elegans Models of Parkinson's Disease. The Journal of Neuroscience. 2017; 37: 11085–11100.

[9] Grassi D, Howard S, Zhou M, Diaz-Perez N, Urban NT, Guerrero-Given D, *et al*. Identification of a highly neurotoxic alpha-synuclein species inducing mitochondrial damage and mitophagy in Parkinson's disease. Proceedings of the National Academy of Sciences of the United States of America. 2018; 115: E2634–E2643.

[10] Naresh NU, Haynes CM. Signaling and Regulation of the Mitochondrial Unfolded Protein Response. Cold Spring Harbor Perspectives in Biology. 2019; 11: a033944.

[11] Beck JS, Mufson EJ, Counts SE. Evidence for Mitochondrial UPR Gene Activation in Familial and Sporadic Alzheimer's Disease. Current Alzheimer Research. 2016; 13: 610–614.

[12] Burbulla LF, Schelling C, Kato H, Rapaport D, Woitalla D, Schiesling C, *et al*. Dissecting the role of the mitochondrial chaperone mortalin in Parkinson's disease: functional impact of disease-related variants on mitochondrial homeostasis. Human Molecular Genetics. 2010; 19: 4437–4452.

[13] Xicoy H, Wieringa B, Martens GJM. The SH-SY5Y cell line in Parkinson's disease research: a systematic review. Molecular Neurodegeneration. 2017; 12: 10.

[14] Abu-Jamous B, Kelly S. Clust: automatic extraction of optimal co-expressed gene clusters from gene expression data. Genome Biology. 2018; 19: 172.

[15] Langfelder P, Horvath S. WGCNA: an R package for weighted correlation network analysis. BMC Bioinformatics. 2008; 9: 559.

[16] Freire C, Amaya E, Gil F, Fernández MF, Murcia M, Llop S, *et al*. Prenatal co-exposure to neurotoxic metals and neurodevelopment in preschool children: the Environment and Childhood (INMA) Project. The Science of the Total Environment. 2018; 621: 340–351.

[17] Cai Y, Shen H, Weng H, Wang Y, Cai G, Chen X, *et al*. Overexpression of PGC-1alpha influences the mitochondrial unfolded protein response (mtUPR) induced by MPP(+) in human SH-SY5Y neuroblastoma cells. Scientific Reports. 2020; 10: 10444.

[18] Guilarte TR, Burton NC, Verina T, Prabhu VV, Becker KG, Syversen T, *et al*. Increased APLP1 expression and neurodegeneration in the frontal cortex of manganese-exposed non-human primates. Journal of Neurochemistry. 2008; 105: 1948–1959.

[19] Song D, Ma J, Chen L, Guo C, Zhang Y, Chen T, *et al*. FOXO3 promoted mitophagy via nuclear retention induced by manganese chloride in SH-SY5Y cells. Metallomics. 2017; 9: 1251–1259.

[20] Higashi Y, Asanuma M, Miyazaki I, Hattori N, Mizuno Y, Ogawa N. Parkin attenuates manganese-induced dopaminergic cell death. Journal of Neurochemistry. 2004; 89: 1490–1497.

[21] Shen Y, Ding M, Xie Z, Liu X, Yang H, Jin S, *et al*. Activation of mitochondrial unfolded protein response in SHSY5Y expressing APP cells and APP/PS1 mice. Frontiers in Cellular Neuroscience. 2020; 13: 568.

[22] Krishna A, Biryukov M, Trefois C, Antony PMA, Hussong R, Lin J, *et al*. Systems genomics evaluation of the SH-SY5Y neuroblastoma cell line as a model for Parkinson's disease. BMC Genomics. 2014; 15: 1154.

[23] Wadgaonkar P, Chen F. Connections between endoplasmic reticulum stress-associated unfolded protein response, mitochondria, and autophagy in arsenic-induced carcinogenesis. Seminars in Cancer Biology. 2021; 76: 258–266.

[24] Ji T, Zhang X, Xin Z, Xu B, Jin Z, Wu J, *et al*. Does perturbation in the mitochondrial protein folding pave the way for neurodegeneration diseases? Ageing Research Reviews. 2020; 57: 100997.

[25] Hu D, Liu Z, Qi X. UPR(mt) activation protects against MPP(+)-induced toxicity in a cell culture model of Parkinson's disease. Biochemical and Biophysical Research Communications. 2021; 569: 17–22.

[26] Lin Y, Schulz AM, Pellegrino MW, Lu Y, Shaham S, Haynes CM. Maintenance and propagation of a deleterious mitochondrial genome by the mitochondrial unfolded protein response. Nature. 2016; 533: 416–419.

[27] Liu M, Yu S, Wang J, Qiao J, Liu Y, Wang S, *et al*. Ginseng protein protects against mitochondrial dysfunction and neurodegeneration by inducing mitochondrial unfolded protein response in Drosophila melanogaster PINK1 model of Parkinson's disease. Journal of Ethnopharmacology. 2020; 247: 112213.

[28] Cooper JF, Machiela E, Dues DJ, Spielbauer KK, Senchuk MM, Van Raamsdonk JM. Activation of the mitochondrial unfolded protein response promotes longevity and dopamine neuron survival in Parkinson's disease models. Scientific Reports. 2017; 7: 16441.

[29] Strauss KM, Martins LM, Plun-Favreau H, Marx FP, Kautzmann S, Berg D, *et al*. Loss of function mutations in the gene encoding Omi/HtrA2 in Parkinson's disease. Human Molecular Genetics. 2005; 14: 2099–2111.

[30] Evinova A, Hatokova Z, Tatarkova Z, Brodnanova M, Dibdiakova K, Racay P. Endoplasmic reticulum stress induces mitochondrial dysfunction but not mitochondrial unfolded protein response in SH-SY5Y cells. Molecular and Cellular Biochemistry. 2022; 477: 965–975.

[31] Liu C, Yan D, Wang C, Ma Z, Deng Y, Liu W, *et al*. IRE1 signaling pathway mediates protective autophagic response against manganese-induced neuronal apoptosis in vivo and in vitro. Science of the Total Environment. 2020; 712: 136480.

[32] Santarelli R, Arteni AMB, Gilardini Montani MS, Romeo MA, Gaeta A, Gonnella R, *et al*. KSHV dysregulates bulk macroautophagy, mitophagy and UPR to promote endothelial to mesenchymal transition and CCL2 release, key events in viral-driven sarcomagenesis. International Journal of Cancer. 2020; 147: 3500–3510.

[33] Kirkley KS, Popichak KA, Afzali MF, Legare ME, Tjalkens RB. Microglia amplify inflammatory activation of astrocytes in manganese neurotoxicity. Journal of Neuroinflammation. 2017; 14: 99.

[34] Forsström S, Jackson CB, Carroll CJ, Kuronen M, Pirinen E, Pradhan S, *et al*. Fibroblast Growth Factor 21 Drives Dynamics of Local and Systemic Stress Responses in Mitochondrial Myopathy with mtDNA Deletions. Cell Metabolism. 2019; 30: 1040–1054.e7.

[35] Goard CA, Schimmer AD. Mitochondrial matrix proteases as novel therapeutic targets in malignancy. Oncogene. 2014; 33: 2690–2699.

[36] Avila DS, Benedetto A, Au C, Bornhorst J, Aschner M. Involvement of heat shock proteins on Mn-induced toxicity in Caenorhabditis elegans. BMC Pharmacology & Toxicology. 2016; 17: 54.

[37] Seo YA, Li Y, Wessling-Resnick M. Iron depletion increases manganese uptake and potentiates apoptosis through ER stress. Neurotoxicology. 2013; 38: 67–73.

[38] Wang T, Li X, Yang D, Zhang H, Zhao P, Fu J, *et al*. ER stress and ER stress-mediated apoptosis are involved in manganese-induced neurotoxicity in the rat striatum in vivo. NeuroToxicology. 2015; 48: 109–119.